J Geod (2009) 83:263–275
DOI 10.1007/s00190-008-0266-1

ORIGINAL ARTICLE

The IGS VTEC maps: a reliable source of ionospheric information since 1998

M. Hernández-Pajares · J. M. Juan · J. Sanz · R. Orus · A. Garcia-Rigo · J. Feltens · A. Komjathy · S. C. Schaer · A. Krankowski

Received: 12 February 2008 / Accepted: 25 August 2008
© Springer-Verlag 2008

Abstract The International GNSS Service (IGS) Working Group on Ionosphere was created in 1998. Since then, the Scientific community behind IGS, in particular CODE, ESA, JPL and UPC, have been continuosly contributing to reliable IGS combined vertical total electron content (VTEC) maps in both rapid and final schedules. The details on how these products are being generated, performance numbers, proposed improvement as far as VTEC evolution trends during near one Solar Cycle, are summarized in this paper. The confirmation of (1) the good performance of the IGS combined VTEC maps, and (2) the characteristic VTEC variability periods, are two main results of this work.

Keywords GPS · Ionospheric VTEC maps · IGS · GNSS

M. Hernández-Pajares (✉) · J. M. Juan · J. Sanz · A. Garcia-Rigo
gAGE/UPC Mod C3 Campus Nord, Jordi Girona 1-3,
08034 Barcelona, Spain
e-mail: manuel@mat.upc.es; manuel@ma4.upc.edu

R. Orus
Propagation Section, ESTEC/ESA, Nordwijk,
The Netherlands

J. Feltens
ESOC/ESA, Darmstadt, Germany

A. Komjathy
JPL/NASA, Pasadena, CA, USA

S. C. Schaer
CODE/swisstopo, Bern/Wabern, Switzerland

A. Krankowski
UWM at Olsztyn, Olsztyn, Poland

1 Introduction

The computation of reliable global maps of vertical total electron content of the Ionosphere (Vertical TEC or VTEC maps) is at the same time an useful and challenging goal. Useful because, in both Science and Technology fields, they can provide valuable information concerning space weather events, empirical model predictions, and user navigation improvement, among others (see for example Coster and Komjathy 2008; Bilitza 2001; Hernández-Pajares et al. 2000). Challenging because, at global scale, there are important parts of the Ionosphere which are not illuminated by any close Global Navigation Satellite Systems (GNSS) satellite-to-receiver ray. This is due to the current lack of GNSS ground receivers, especially over the Oceans and in the Southern Hemisphere, among other regions.

Moreover, the Inverse Problem to retrieve such VTEC maps from the Slant TEC (STEC) measurements is not straightforward. This is because these measurements do not directly provide the STEC (the carrier phases are affected by the ambiguity term, and the pseudoranges by the inter-frequency code bias, see for instance Hernández-Pajares et al. 2008). In addition, conversion of VTEC is complicated by the variation of the electron content in space and time, with special difficulties close to the Equatorial Anomalies, and/or during Ionospheric storms.

The Ionosphere Working Group of the International GNSS Service (Iono-WG) was created in 1998 (see Feltens and Schaer 1998) with the goal of generating reliable VTEC maps. A similar approach to those used by older IGS Working Groups that provide reliable GNSS products such as satellite orbits and clocks was taken: individual products (in our case global VTEC maps) were independently computed (software and hardware) by different computation centers, are ranked and combined with the corresponding weight in

terms of single IGS global VTEC maps. The different maps are computed by the so called Ionospheric Associate Analysis Centers (IAACs), the corresponding ranking is computed by the so called Ionospheric Associated Evaluation Centers (IAECs) and the IGS-combined product is produced by the so called Ionospheric Associate Combination Center (IACC). This has been done under the direct responsibility of the Iono-WG chairman: Dr. Joachim Feltens from European Space Operations Centers from the European Space Agency, (ESOC/ESA, see http://www.esa.int/SPECIALS/ESOC/index.html) since 1998–2002, the first author of this manuscript from the research group of Astronomy and Geomatics, Technical University of Catalonia, gAGE/UPC (http://www.gage.es) since 2002–2007, and Dr. Andrzej Krankowski from University of Warmia and Mazury in Olsztyn, UWM (http://www.uwm.edu.pl/en/), since 2007). Finally a validation with independent sources of VTEC data is performed by the Ionospheric Associated Validation Centers (IAVCs).

This paper will describe details on how the IGS VTEC maps are generated, and will provide an update of the corresponding performances with some representative snapshots (including the inter-frequency biases as secondary product). In addition, the product usage, the main VTEC evolution trends during near one Solar cycle, and potential future improvements will be discussed. In particular we will show the main characteristics of VTEC variation in order to better understand its typical periodic variability. And last but not the least, with this manuscript the authors intend to divulgate the availability of these reliable IGS VTEC maps for scientific or application usages.

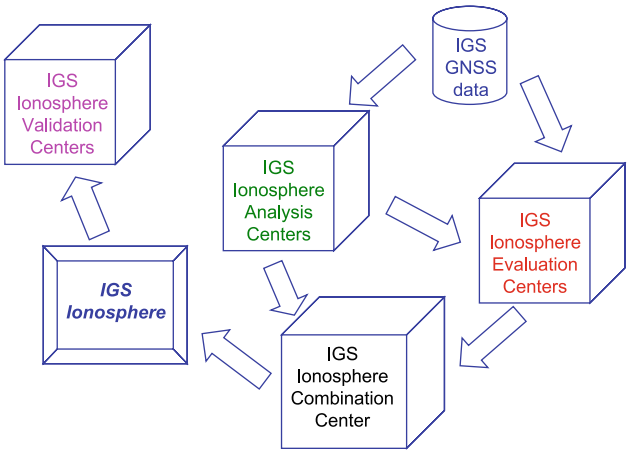

Fig. 1 Diagram showing the data flow required to generate the IGS VTEC maps

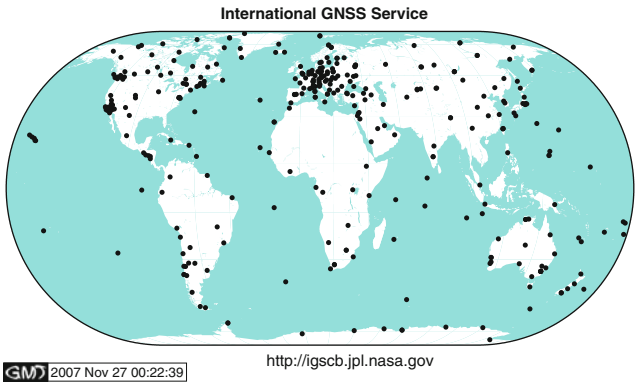

Fig. 2 Map showing the distribution of IGS receivers (as of 26 November 2007)

2 From raw data to ionospheric maps

In order to generate the combined VTEC maps several steps are needed, as it is represented in Fig. 1:

Raw GNSS data measurements: They are provided by the IGS GNSS ground network. Presently IGS manages a network of 384 stations, many of them covering continental North Hemisphere (as of 26 November, 2007; see Fig. 2 and details in Dow et al. 2005 and International GNSS Service Central bureau, http://www.igs.org).

Independent computation of VTEC maps by the analysis centers: Currently[1] four IAACs contribute with their rapid and final VTEC maps to the IGS products: CODE (Center for Orbit Determination in Europe, http://www.aiub.unibe.ch/content/research/gnss/code___research/index_eng.html), ESA, JPL (Jet Propulsion Laboratory, http://iono.jpl.nasa.gov/), and UPC. They are computing the global distribution of TEC independently and with different approaches (see corresponding details of their techniques in Schaer 1999; Feltens 1998, 2007; Mannucci et al. 1998; Hernández-Pajares et al. 1999), including the additional usage of GLONASS (from Russian *Global'naya Navigatsionnaya Sputnikovaya Sistema*, http://www.glonass-ianc.rsa.ru/pls/htmldb/f?p=202:1:2602323727446128426) data in the case of CODE.[2] As a matter of example, you can see in Fig. 3 the layout of a typical approach to compute global VTEC maps from GNSS data (it corresponds to UPC approach).

In order to make feasible the generation of a combined IGS ionospheric product, the IAACs agreed on providing their maps in IONEX format (IONosphere map EXchange

[1] From 1998 to 2003 NRCan, Natural Resources Canada (formerly EMR) was also contributing as IAAC, see corresponding technique in Gao et al. (1994).

[2] It is, for the time being, the only ionosphere analysis center generating GPS and GLONASS combined GIM/DCB products, see Schaer (2003) for details.

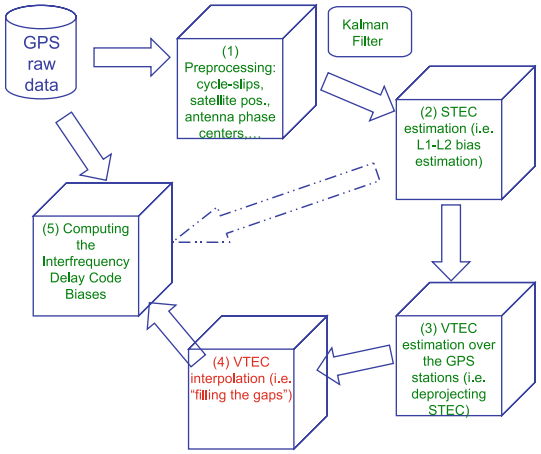

Fig. 3 Diagram showing the main typical steps on computing global VTEC maps (source: UPC)

format, see Feltens and Schaer 1998), with a resolution of 2 h, 5° and 2.5° in time, longitude and latitude respectively (you can see a typical example of IAAC maps snapshots in Fig. 4, corresponding to a day—13 December 2003—with intermediate values of electron content within the last Solar Cycle).

Evaluation of the VTEC maps provided by the analysis centers: Currently UPC is providing the evaluation of the different global VTEC maps, from the point of view of how they are able to reproduce observed STEC variations. This is done by computing the weights for their combination from the inverse root mean square of errors on reproducing observed STEC variations. The observed STEC variations are very precise values (more accurate than 0.1 TECU),[3] obtained from carrier phase observations for a certain subset of test stations (i.e. by using the so called "Self-Consistency Test", see example in Fig. 5 and details for instance in Orus et al. 2007).

Combination of the VTEC maps provided by the analysis centers: The combined IGS maps are obtained as a simple weighted mean of the available IAAC VTEC maps, by using the values provided by the Evaluation Center in previous step (Fig. 6 shows an example of IGS VTEC and corresponding Root Mean Square (RMS) snapshots, after combining maps of Fig. 4 and taking into account the evaluation involving Fig. 5).

A similar process is performed for combining the Delay Code Biases[4] (DCBs) estimates for transmitters (Global Positioning System, GPS, http://www.gps.gov-satellites) and receivers[5] (see for instance Wilson and Mannucci 1993; Sardon et al. 1994). Considering the same example day (347 of year 2003), Fig. 7 shows the satellite DCB estimations for each IAAC and for the combined IGS values, taking into account that each DCB dataset is referred to the corresponding satellite averaged value. Typical values between −4 and +5 nanoseconds, and discrepancies at the level of few tenths of ns (see also Hernández-Pajares 2004), can be seen in such a plot. On the other hand the GPS receiver DCBs are plotted in Fig. 8 in terms of the latitude, for the 44 common stations, with the final estimates provided by three centers on the same day (COD, JPL and UPC with associated final product labels CODG, JPLG and UPCG) together with the corresponding final combined IGS values (labelled as IGSG). Typical values ranging from −20 to +15 nanoseconds can be seen, with a variability up to few nanoseconds, also coincident with the more detailed study in the above mentioned reference Hernández-Pajares (2004). Such variability between different estimations is larger at low latitude, as it can be appreciated in the deviation plot (Fig. 9). This is coincident with the higher electron density and VTEC variability in such a region, producing larger errors and discrepancies between IAAC computation strategies (as it can be seen in the snapshots of Fig. 4 and RMS plots of combined VTEC maps in Fig. 6). Regarding to mid latitudes, a relative bias can be clearly seen between IAACs at North Hemisphere (where more receivers are available, in North America and Europe): The UPCG receiver DCBs fall 0.2–0.4 nanoseconds above the CODG ones, and UPCG values are about 0.2–0.4 nanoseconds greater than JPL receiver DCBS at North mid latitude regions. These small but clear biases are consistent, for JPL and UPC, with the corresponding VTEC biases of about 2 TECUs (UPC lower than JPL, see validation below at Fig. 12 for latitude bin of +60°), versus the reversal receiver DCB biases of about 0.4 nanoseconds = 12 cm of $L_I \equiv L_1 - L_2 = 1.2$ TECU, being L_1 and L_2 the carrier phases in length units of both GPS carriers at $f_1 = 1575.42$ MHz and $f_2 = 1227.60$ MHz respectively. This is a consistent result because of both unknowns, VTEC and DCBs, are estimated from the common ionospheric data (geometric-free combination of pseudoranges $P_I = P_4$, and carrier phases $L_I = L_4$, see any of the above mentioned references dealing with the IAAC computation strategies). In Figs. 7, 8 and 9 the weighted values of IGS DCBs are

[3] 1 TEC Unit ≡1 TECU =10^{16} electrons/m^2

[4] As it is well know there is a certain lack of synchronization–typically several nanoseconds–between GPS f_1 and f_2 signals within the transmitters and receivers, affecting directly to pseudorange measurements: these are the so called delay code biases, DCBs, for both transmitters and satellites, which values are defined assuming zero for the ionospheric-free combination of pseudoranges P1 and P2.

[5] In this case the weighting is done, for each IAAC, from its RMS regarding to the plain between-IAACs-average values, for the different satellite DCBs.

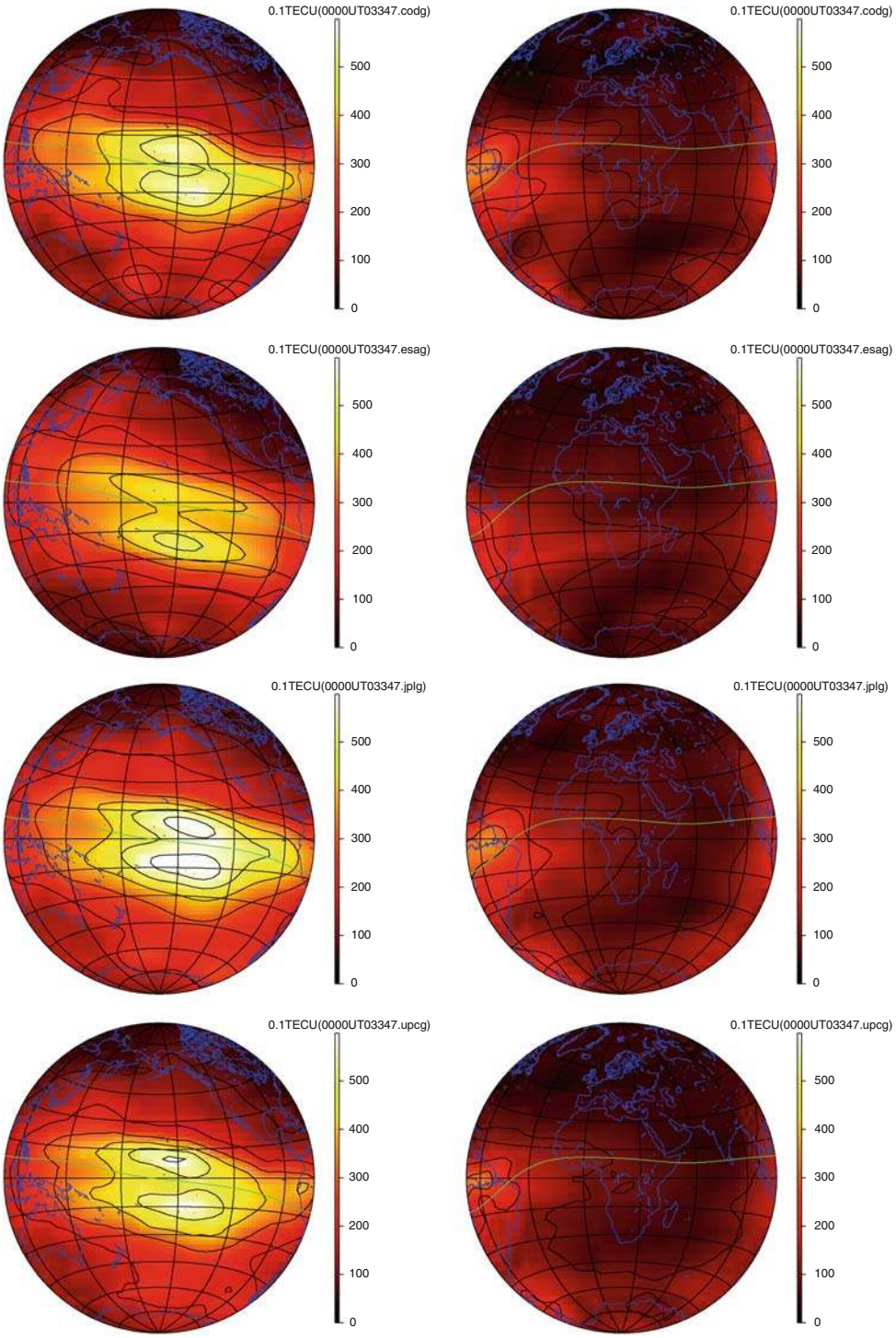

Fig. 4 Example of IAAC VTEC maps snapshots, for day 347 (13 Dec) of 2003, at 00UT. Every *row*, from *top* to *bottom*, corresponds to CODE, ESA, JPL and UPC. The units for all maps are tenths of a TECU

also shown for the sake of completeness, behaving in the logical way due to its combined origin.

Validation of the IGS VTEC map by comparing it with an independent source of VTEC: The reference VTEC values are provided by dual frequency altimeters on board TOPEX satellite (up to 2003, see http://sealevel.jpl.nasa.gov/mission/topex.html) and JASON satellite (from 2003 so far, see http://sealevel.jpl.nasa.gov/mission/jason-1.html), and ENVISAT (from 2003 so far, see http://envisat.esa.int/). Because the altimeters are working over Oceans, this comparison can be considered as a pessimistic determination of the global VTEC map actual errors. Indeed, in such regions there are few ground based GNSS receivers, and as a consequence, most part

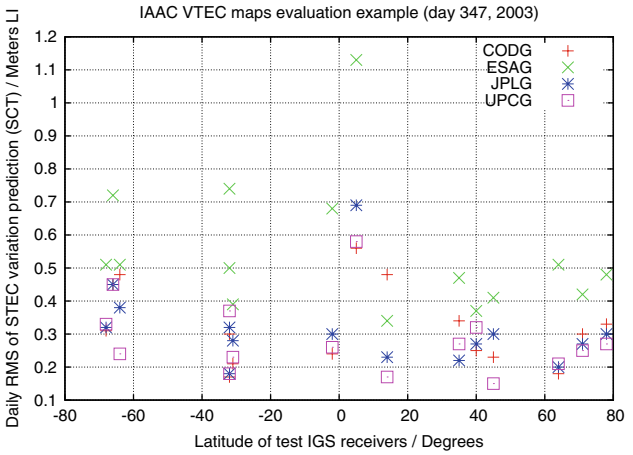

Fig. 5 Example of evaluation of IAAC VTEC maps: Daily RMS of the STEC variation prediction (Self-Consistency Test) from different IAAC Global VTEC maps (CODE, ESA, JPL and UPC), in terms of the test station latitude (Day 347 of 2003). The units are meters of ionospheric carrier phase combination, $L_I \equiv L_4$, being 1 meter of $L_I = 9.52$ TECU

of the provided information by the VTEC global maps is based on interpolation. Presently there are two IAVCs: JPL and ESOC/ESA, providing JASON and ENVISAT validations. As a matter of example, in Fig. 10 some comparisons with JASON data are shown, corresponding to IGS final VTEC maps, including that of Fig. 6. In Fig. 11 the full one-to-one comparison for such a day can be seen, showing that, in spite an overall agreement is typically reached, a certain GNSS underestimation can be found for high VTEC values, corresponding to altimeter passes over the equatorial peaks of electron content. Moreover, the corresponding JASON vs GNSS VTEC bias can be seen in Fig. 12, which shows the relative biases between IAAC models, as far as the typical "U" shape in terms of the latitude, compatible with the plasmaspheric signal of up to few TECU at low latitudes (see Hernández-Pajares 2004, for a more significant plasmaspheric signature). In this same figure, the daily Standard Deviation regarding to JASON VTEC is indicated in the labels, showing the typical good behaviour of the combined IGSG map (similar or still better than the best individual maps). Beyond these examples, a more significant comparison with final IGS VTEC maps can be found below.

Broadcasting of VTEC maps: Once the IGS VTEC maps are computed they are placed in the main IGS distribution server at cddis.gsfc.nasa.gov. They can be reached from ftp://cddis.gsfc.nasa.gov/gps/products/ionex/YEAR/DOY, the final maps after about 9–16 days as igsgDOY0.YYi.Z, and rapid maps after 1–2 days as igrgDOY0.YYi.Z, being DOY the Day Of Year, and YY the last two digits of the year (a table containing a complete list of IGS products, as far as servers providing them, can be found in http://igs.org/components/prods.html). The corresponding IAAC maps are also available, as far as final assessment and altimetric validation data.

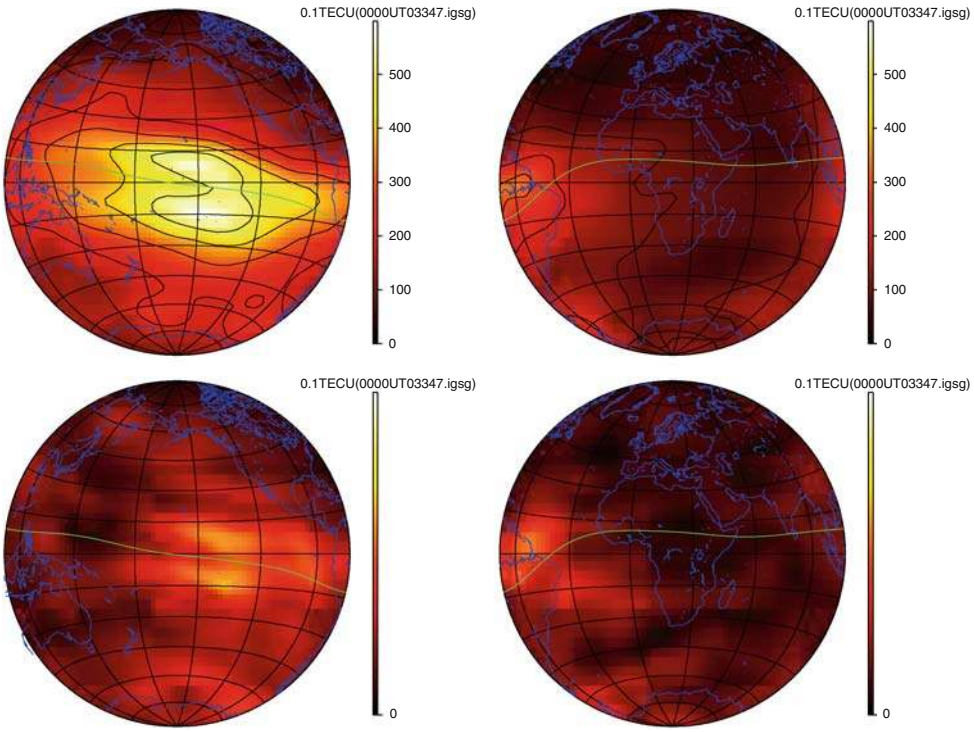

Fig. 6 Example of IAAC VTEC maps snapshots (*top row*), for day 347 (13 Dec) of 2003, at 00UT. The *bottom row* contains the corresponding RMS maps. The units for all maps are tenths of a TECU. The scale ranges from 0 to 60 TECU in the VTEC maps, and from 0 to 6 TECU units in the RMS maps

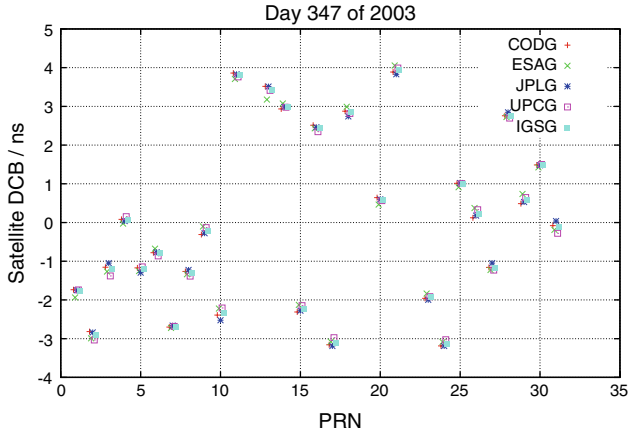

Fig. 7 GPS Satellite Delay Code Biases in nanoseconds, in terms of the corresponding PRN id, for the IAACs and the weighted IGSG value (Day 347 of 2003)

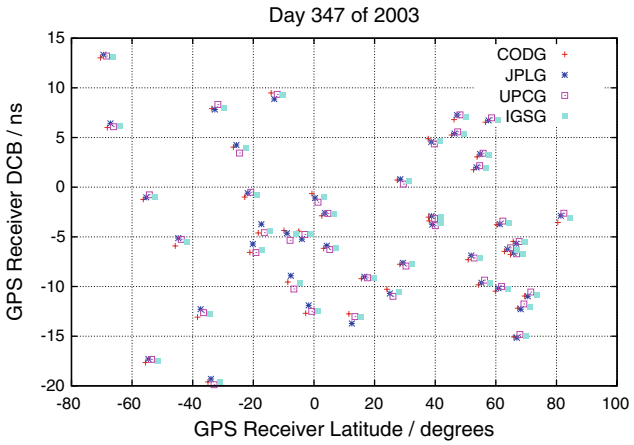

Fig. 8 GPS Receiver Delay Code Biases in nanoseconds, in terms of the corresponding receiver latitude for the IAACs and the weighted IGSG value (Day 347 of 2003)

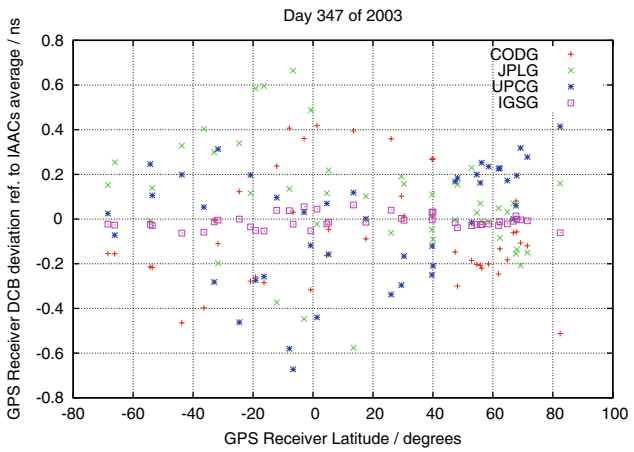

Fig. 9 GPS Receiver Delay Code Biases deviation (regarding to the different IAACs and IGSG average) in nanoseconds, in terms of the corresponding receiver latitude for the IAACs and the weighted IGSG value (Day 347 of 2003)

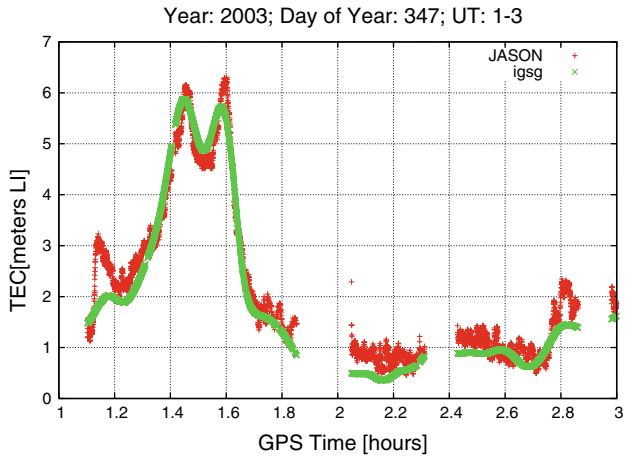

Fig. 10 Example of validation of IGS VTEC map over the Dual frequency JASON Altimeter footprint during 01-03UT, day 347 of 2003: Directly measured altimeter VTEC (*red plus symbol*) vs. VTEC deduced from IGS global maps (*green crosses*). Note: the altimeter measurements are just slightly smoothed before being compared (in this case by an sliding window containing 16 consecutive observations, during a time span of about 16 s)

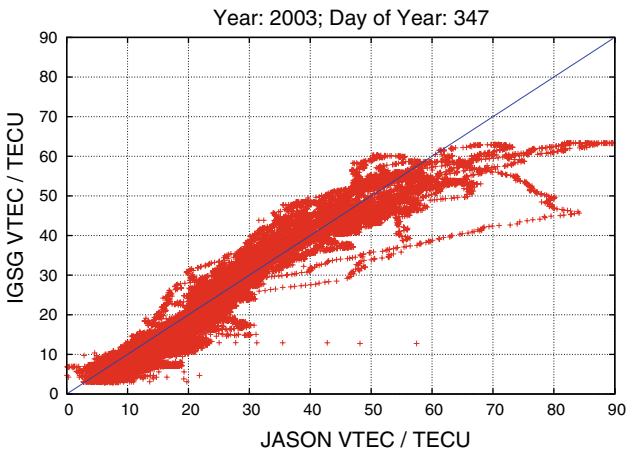

Fig. 11 IGS VTEC versus JASON Altimeter VTEC during the whole day 347 of 2003

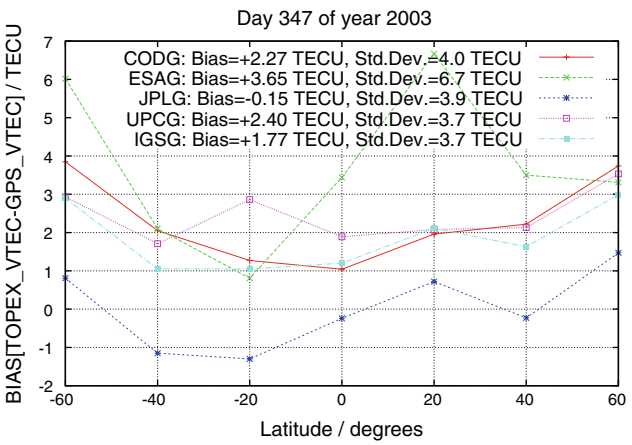

Fig. 12 JASON versus IGS bias (average of JASON minus GNSS VTEC) in terms of latitude bins of 20° (day 347 of 2003)

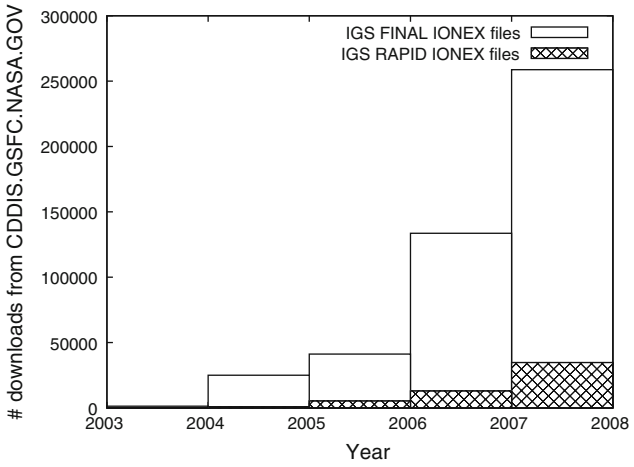

Fig. 13 IGS IONEX usage statistics for both final (IGSG) and rapid (IGRG) VTEC maps: downloads from main server only (cddis.gsfc.nasa.gov)

It has to be pointed out that the evolution of usage has maintained a continuous growth (see for example Fig. 13 considering only the statistics of the main IGS server (Crustal Dynamics Data Information System, CDDIS, http://cddis.nasa.gov/ftpgpsstruct.html)—no IGS mirrors nor UPC servers included-).

3 Overall validation of VTEC maps during more than 9 years of IGS final VTEC maps

In order to provide significant performance numbers of IGS VTEC maps, the comparison between the interpolated VTEC value from IGS final maps and the direct altimeter (TOPEX or JASON) measurement is shown in Fig. 14. This comprises the more recent period since day 349, 2002 up to end 2007 (after improvement of several IAAC VTEC mapping techniques), in terms of the cumulative distribution function of the GNSS-Altimeter discrepancies. The good agreement can be seen in such worst case scenario (over the Oceans, typically far from GNSS receivers) which is in general equal or better than the best performance of each individual IAAC VTEC map (see in the same Fig. 14, the corresponding study for CODG, ESAG, JPLG and UPCG). The better behaviour is quantified and confirmed in Table 1, for instance in terms of the Standard Deviation or the corresponding error ratio (less than 20%), 3rd and 7th columns respectively in Table 1.

Regarding to the satellite DCBs, the typical evolution of a satellite DCB (in this case for PRN01,[6] see Fig. 15) since the beginning of Iono-WG activities can be seen, for the four presently active IAACs. Three aspects can be remarked: (1) the agreement of the different determinations during the last years (notice they are shifted for better visibility), (2) the range scale at the level of few nanoseconds in about 10 years, and (3) some periodic variations observed in several centers (such as those yearly variations in CODE and UPC DCBs during Solar Max conditions) which could be related with TEC variations[7] (see below). Beyond these variations, it has to be taken into account that most part of long term and small discontinuity jumps are just associated to changes in the GPS Constellation, producing the corresponding shift in the common DCB reference (the average values of satellite DCBs). Beyond that, it can be seen in Table 2 that the agreement between different estimates is at the level of 0.1 ns during 2007 (relative *errors* for GPS satellite DCBs of about 4–7%). The corresponding comparison, regarding to different subsets of available receiver DCBs, are also included in Table 3, showing discrepancies at the level of 0.5–0.7 ns. Moreover, and as a matter of example, the DCB evolution for two typical receivers (ALBH at mid latitude and DGAR at low latitude) is represented in Fig. 16 for the last years (final IGS combination). It can be appreciated the lower quality of the determination at low latitude, associated with the higher difficulties on TEC modelling under higher gradients associated to the Ionospheric Equatorial Anomalies.[8]

The last, but not the least: since the end of 2003, a rapid IGS VTEC product (mentioned in previous sections) has been generated in a daily basis with latencies below 24 h. This improves significantly the availability of IGS global VTEC maps compared with the final IGS product, with latencies (on a weekly basis) up to 10 to 12 days. The only apriori drawback of the rapid product is the availability of slightly less stations, which produces a small decrease of performance of about 5–7%, as it can be seen for year 2007 in the one-to-one plot of Fig. 17. This good agreement is also maintained for satellite and receiver DCBs, with discrepancies of about 4 and 6% during 2007 (see Tables 2 and 3).

4 Evolution of global electron content during more than 9 years of IGS final VTEC maps

Once the good quality of combined IGS VTEC maps has been shown in last section, we can focus on the evolution of

[6] PRN is an acronym for Pseudo Random Number, the identifier for every active GPS satellite.

[7] The relationship between DCB estimation and electron content can be specially significant with the far plasmaspheric component, which appears affected by a deprojection factor—mapping function—close to 1, similarly to the DCB unknown coefficient in the model jacobian to be solved for.

[8] Other potential source to explain this different behaviour, a different level of pseudorange measurement noise, should be discarded because they share a similar level of measurement error: 2 TECU peak-to-peak in ionospheric pseudorange combination.

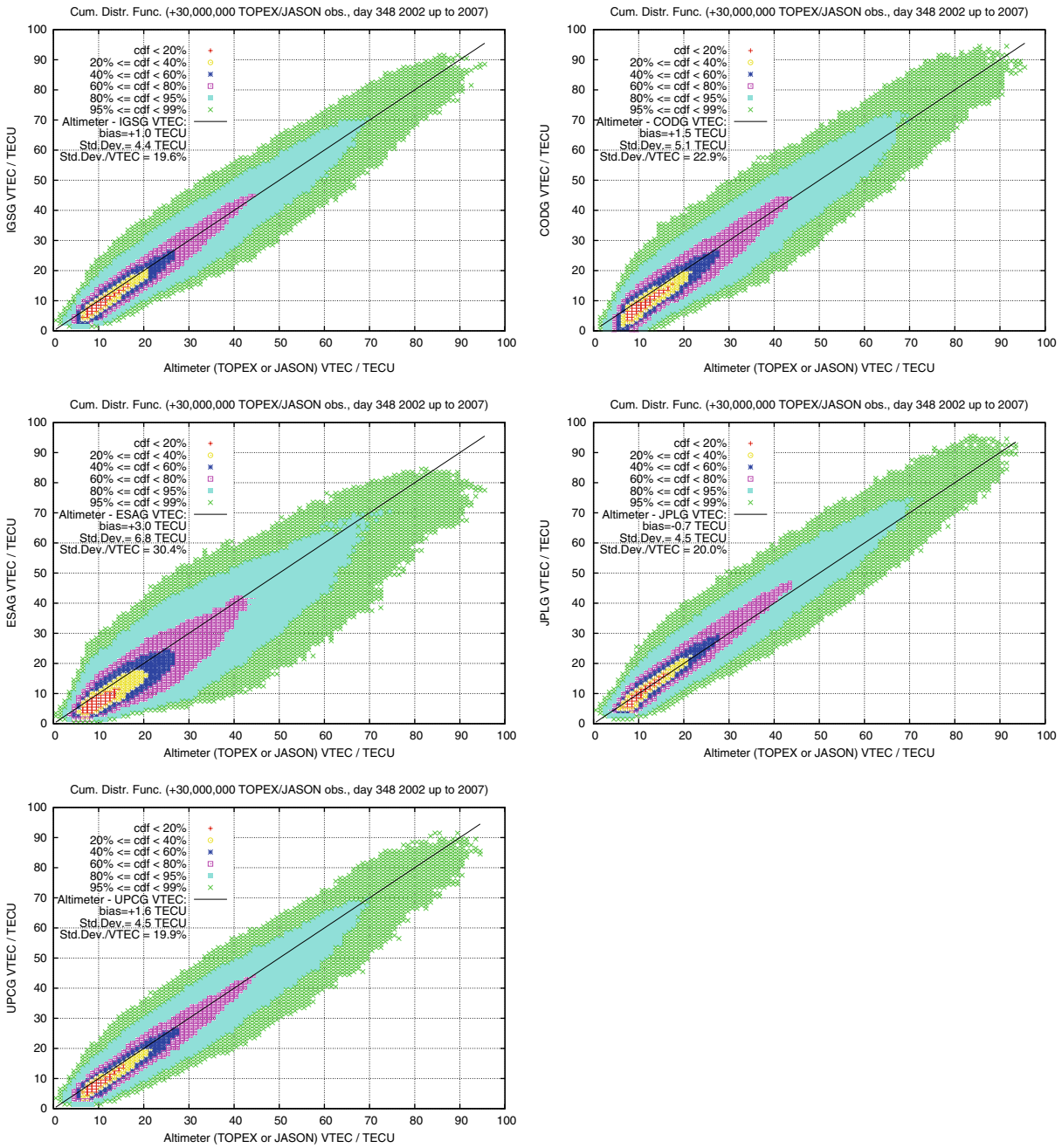

Fig. 14 Cumulative Distribution Function of VTEC discrepancy values provided by final VTEC maps (*vertical axis*) regarding to the VTEC values, directly observed by the TOPEX/JASON altimeters (*horizontal axis*), during the period day 349 2002 to end of 2007 (+30,000,000 observations): From left to right, from top to bottom: IGSG, CODG, ESAG, JPLG and UPCG

the Global Electron Content, GEC. This ionospheric index is computed from the integration of the overall VTEC maps on the overall Ionosphere surface (in which the free electrons distribution is approximated) and was proposed as Ionospheric index in Astafyeva et al. 2006 (the associated unit is called Global Electron Content Unit, or GECU, defined as 10^{32} electron/m^2). It is equivalent to the mean global VTEC, previously defined and studied in Schaer (1999).

In Fig. 18 the consistency of the GEC, computed by integrating the overall IAAC VTEC maps on the overall Ionosphere surface, is shown since the IGS ionospheric productions kickoff, 1 June 1998. The corresponding difference relative to IGSG GEC is also included in Fig. 19 (conveniently shifted for sake of clarity). The compatibility of the different VTEC maps, obtained with different techniques, can be seen again. Only slightly different biases

Table 1 Statistics of the difference TOPEX/JASON VTEC—GNSS VTEC

	Bias TECU	Std. Dev TECU	RMS TECU	VTEC TECU	RMS/VTEC (%)	Std. Dev./VTEC (%)
IGSG	1.00	4.42	4.53	22.48	20.14	19.65
CODG	1.45	5.14	5.35	22.47	23.78	22.89
ESAG	2.96	6.84	7.45	22.47	33.17	30.44
JPLG	−0.72	4.49	4.54	22.49	20.21	19.95
UPCG	1.55	4.46	4.72	22.46	21.03	19.87

Bias, Standard Deviation, RMS, mean VTEC (in TECUs), and error percentages from RMS and Standard Deviation, have been computed from different final VTEC maps: IGSG, CODG, ESAG, JPLG and UPCG (+30,000,000 TOPEX/JASON observations from day 349 2002 until end 2007)

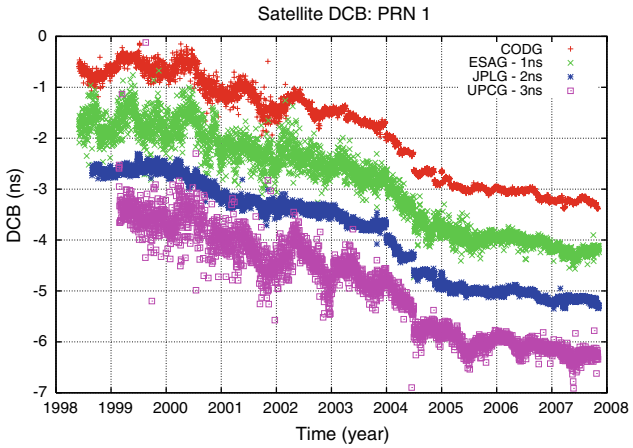

Fig. 15 Evolution of PRN01 DCB for the four presently active IAACs (the different determinations are shifted to facilitate the comparisons)

associated with the intrinsic differences in the data processing and modelling (such as the different mapping function used for estimation) can be seen, as it was already manifested in the validation with altimeter VTEC observations, see Fig. 14 (also pointed out by Afraimovich et al. 2006). The small biases change from time to time, this being likely associated with technique updates from the corresponding analysis centers.

As a first application of this huge database we will look for periodic changes in the electron content evolution, and potential sources of these variations.

It can be seen in Fig. 20 the IGSG GEC evolution. The global signature of the Solar Cycle, as far as the seasonal, and near monthly periods (see zoom at Fig. 21) is evident. This last variation (which will be analyzed below in terms of the Power Spectral Density, PSD) appears mostly correlated with the Solar Flux evolution (see again Figs. 20 and 21).

Thanks to this large observational period of about a decade, many periodic components of the electron content evolution can be studied. In Fig. 22 (log-log plot) the GEC Power Spectral Density can be seen. As it is indicated in the corresponding caption, several PSD peaks can be observed, including the more significant at half year, one year, one and half year, 27 days, one, half, one third, one quarter and one fifth of a day. In particular the 27-days period (peak at 26.79 ± 0.12 days) is quite compatible with the equatorial Solar synodic rotation period (27.28 days), which affects the sunspot groups. This can be seen in corresponding Solar Flux PSD plots in same figure. This corresponds to the correlation observed between GEC with Solar Flux, see Fig. 21), also pointed out by previous authors (see for instance Schaer 1999; Wang et al. 2006 for discussion about this correlation with radio and X-ray solar flux, and Astafyeva et al. (2006) for similar result from GEC). The peaks at 1, 0.5 and 0.33 days

Table 2 Satellite Delay Code Bias agreement between rapid IGS and different final IAAC estimates, regarding to Final IGS (IGSG) values for year 2007

	Bias (ns)	Std. Dev (ns)	RMS (ns)	‖Sat. DCB‖ (ns)	$\frac{\text{RMS}}{\|\text{Sat. DCB}\|}$ (%)	$\frac{\text{Std. Dev.}}{\|\text{Sat. DCB}\|}$ (%)	# Comp.
IGRG	+0.08	0.08	0.10	2.62	4.07	2.89	8722
CODG	+0.08	0.09	0.12	2.61	4.58	3.36	10523
ESAG	+0.04	0.17	0.17	2.67	6.39	6.25	10075
JPLG	+0.08	0.11	0.13	2.61	5.10	4.07	10520
UPCG	+0.07	0.17	0.19	2.61	7.13	6.64	10398

The statistics of the differences, regarding to IGS final (IGSG) Delay Code Biases, include: Bias, Standard Deviation, RMS, mean of DCB absolute values (in ns), error percentages from RMS and Standard Deviation, and number of comparisons. They have been computed from corresponding IONEX file headers

Table 3 Receiver Delay Code Bias agreement between rapid IGS and different final IAAC estimates, regarding to Final IGS (IGSG) values for year 2007 (Notice in last column that the comparison sets can be quite different, depending on availability of the estimates)

	Bias (ns)	Std. Dev (ns)	RMS (ns)	‖Rec. DCB‖ (ns)	$\frac{\text{RMS}}{\|\text{Rec. DCB}\|}$ (%)	$\frac{\text{Std. Dev.}}{\|\text{Rec. DCB}\|}$ (%)	# Comp.
IGRG	−0.04	0.51	0.51	8.00	6.43	6.41	46401
CODG	+0.08	0.19	0.20	8.08	2.48	2.29	52972
ESAG	−0.01	0.70	0.70	8.19	8.59	8.59	54702
JPLG	+0.10	0.69	0.70	8.11	8.64	8.56	48326
UPCG	+0.39	0.68	0.77	5.44	14.20	12.28	13716

The statistics of the differences, regarding to IGS final (IGSG) Delay Code Biases, include: Bias, Standard Deviation, RMS, mean of DCB absolute values (in ns), error percentages from RMS and Standard Deviation, and number of comparisons. They have been computed from corresponding IONEX file headers

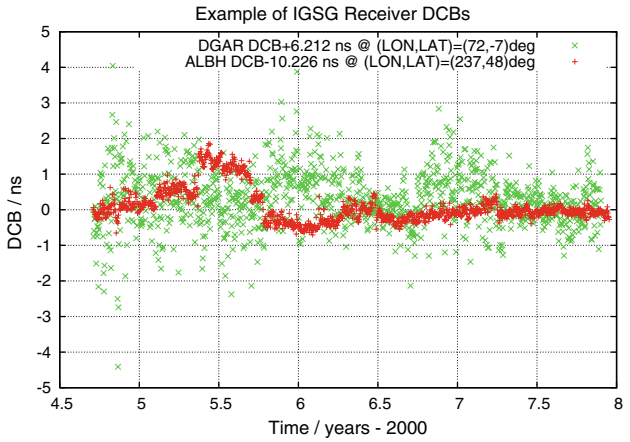

Fig. 16 Recent evolution of Receiver DCB (IGSG determination) for two typical midlatitude and low latitude receivers: ALBH and DGAR

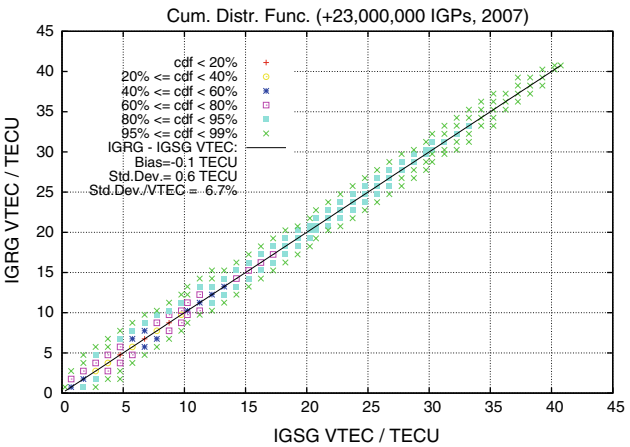

Fig. 17 Cumulative Distribution Function of VTEC values provided by rapid IGS VTEC maps (*vertical axis*) regarding to the final IGS VTEC values (*horizontal axis*), during 2007 (+23,000,000 Ionospheric Grid Values)

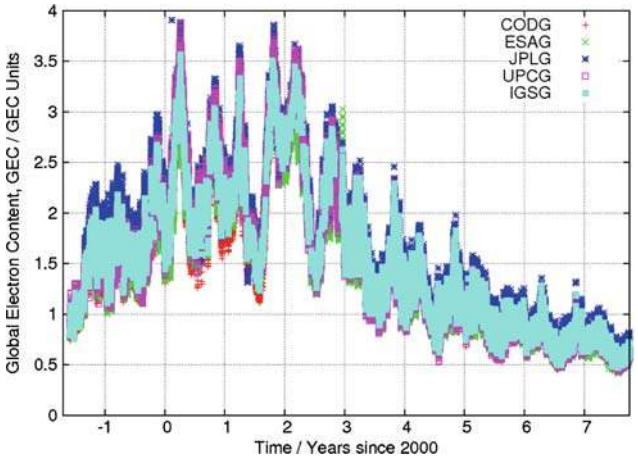

Fig. 18 Global electron content evolution during the availability of IGS Ionospheric products, since 1 June 1998 (source: Final IGS VTEC maps)

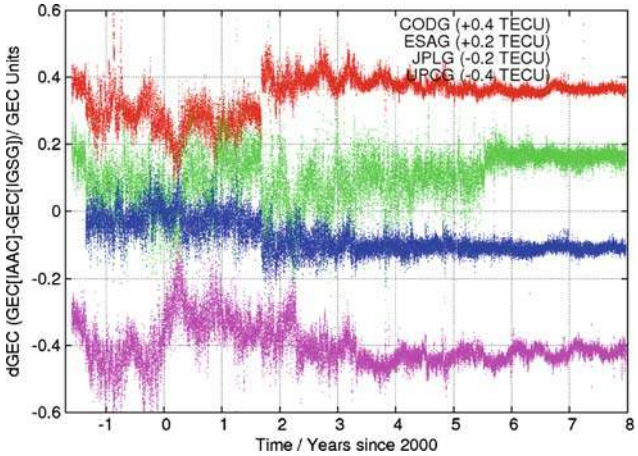

Fig. 19 Evolution of global electron content referred to the IGSG one (source: Final IGS VTEC maps). Notice that the values are shifted for CODG (*red*), ESAG (*green*), JPLG (*blue*), UPCG (*magenta*) by +0.4, +0.2, −0.2 and −0.4 TECUs, respectively, to facilitate the comparisions

can be associated with the diurnal, semidiurnal and terdiurnal tide effects on Ionosphere (see Stening and Fejer 2001; Heelis and Coley 1992; Schaer 1999).

Other peaks can be appreciated, focusing on the interval between 2 and 18 days (see Fig. 23), being the most important one at 14 days (which is still more important for

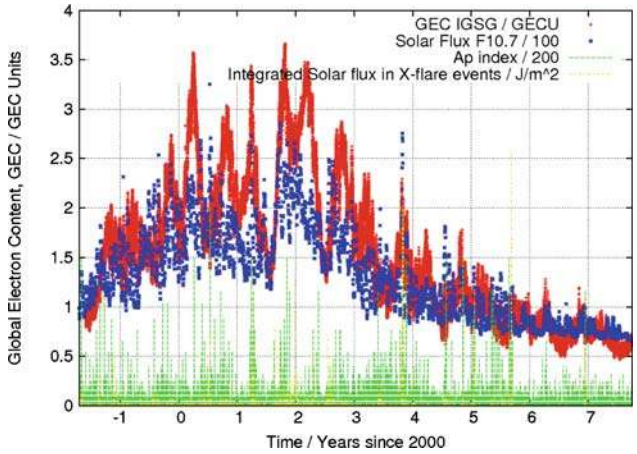

Fig. 20 Global electron content evolution during the availability of IGS Ionospheric products, versus Solar Flux, Ap index and Xray flux, since 1 June 1998 (source: Final IGS VTEC maps)

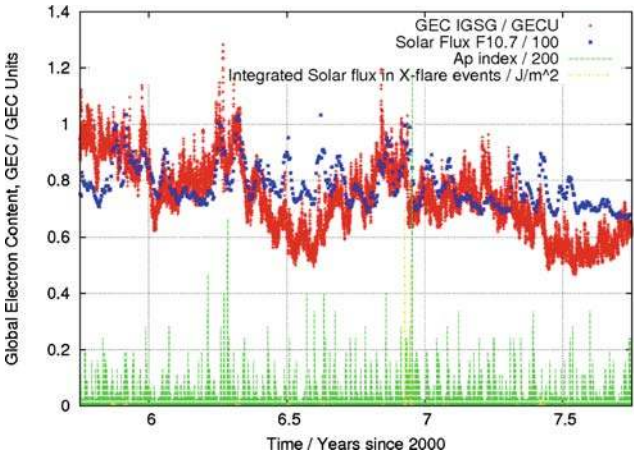

Fig. 21 Global electron content evolution during the availability of IGS Ionospheric products, versus Solar Flux, Ap index and Xray flux: Zoom since end 2005 (source: Final IGS VTEC maps)

night hemisphere). This characteristic GEC period is quite compatible with the lunar semimonthly tide (see for instance Stening et al. 1999 for effects on Ionosphere and Bellanger et al. 2002 for effects on Earth rotation). Other periods such as that at 9 days (and also the less significant period of 5 days), are coincident with periods of planetary wave type oscillations at the Equatorial Ionospheric Anomalies (see Fagundes et al. 2005). In the case of the 9-days period, it is also coincident with the characteristic time for plasmaspheric depletion and successive replenishment following storm activity (see Belehaki et al. 2003).

Finally the VTEC PSD, at a Mid Latitude grid point placed over America, is plotted in Fig. 24, for North and South Mid Latitude, for both Noon and Midnight Local Times. Significant peaks are found at annual, semiannual and Solar rotation periods, also found in GEC and discussed above. Moreover

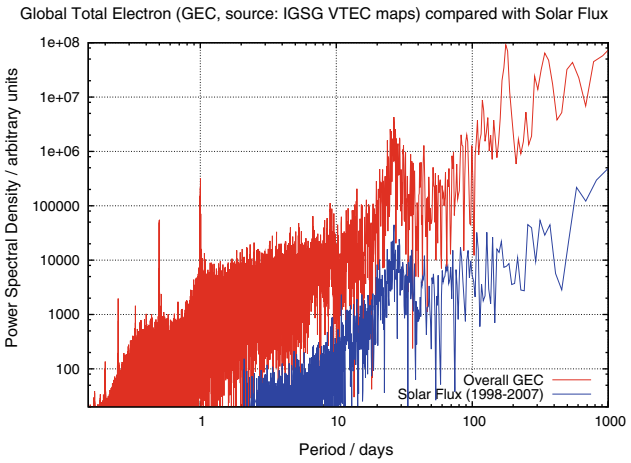

Fig. 22 IGS Final GEC Power Spectral Density in log-log scale (*red line*), corresponding to the availability of IGS final VTEC maps (1 June 1998 until end 2007, the epoch in which this manuscript has been written. The main peaks can be seen, from lower to upper periods, at 0.20 ± 0.00, 0.25 ± 0.00, 0.33 ± 0.00, 0.5 ± 0.00, 1 ± 0.00, 26.79 ± 0.12, 44 ± 0.35, 120 ± 2.64, 180 ± 5.93, 345 ± 21.79 and 551 ± 55.59 days (see more comments in text body). The corresponding result for Solar Flux Series are also plotted for comparison, showing two similar peaks, at periods of 26 and 44 days

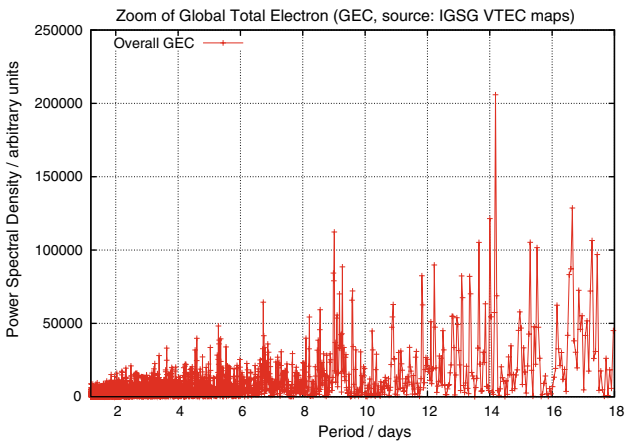

Fig. 23 Zoom in linear scale of IGS Final GEC Power Spectral Density (*red line*) from periods from 2 to 18 days. The peaks in this interval can be seen, from upper to lower intensity, at periods of 14.18 ± 0.04, 16.65 ± 0.05, 9.02 ± 0.01, 6.74 ± 0.01 and 5.30 ± 0.01 days (see more details in body text)

the peaks at 120 days in Noon North, 90 days at Noon South, and 13.6 days also appear.

5 Conclusions and future improvements

In this manuscript we have shown how the IGS VTEC maps, which have been generated without interruption since 1998, are computed, and described their main properties. In particular the improved behaviour in terms of accuracy relative to the individual maps used in the combination has been

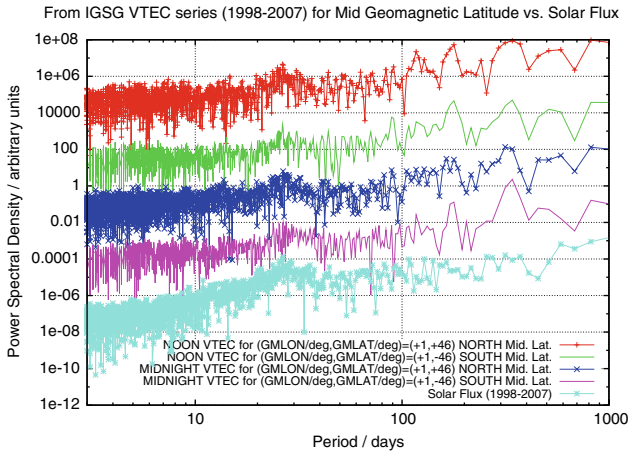

Fig. 24 VTEC PSD for Mid Latitude, compared between North and South Hemisphere at Noon time, and also at Midnight. Significant common peaks are found at 344, 180 and 26 days (this also coincident with Solar Flux). Moreover peaks at 120 days in Noon North, 90 days at Noon South, and 13.6 and 9 days in Midnight North Hemisphere only. Source: final IGS VTEC maps since June 1998

demonstrated. In fact, an upperbound error estimate of 20% (see Table1) is shown since end of 2002 (obtained over the oceans, comparing it with more than 30 million of altimeter VTEC measurements, and neglecting the altimeter errors, which bias -positive- and noise are at the level of few TECU, see for instance Coker et al. 2001). The performance analysis is complemented with the comparison of DCBs (for both GPS satellites and receivers) between individual centers and rapid IGS values, and final IGS DCBs.

At the same time, thanks to the availability of a continuous series of IGS VTEC maps during about 10 years, the main trends of evolution are also summarized in terms of Global Electron Content time series, and the corresponding main spectral features, have been analyzed, confirming results prompted in previous works. The long series of IGS VTEC maps offers a very good source with sufficient spatial and temporal resolution, to get significant spectral results.

On the other hand, future improvements are quite determined by the users needs, which number—as it has been shown above—has significantly increased during the last years. A recent example is that, as a consequence of the recent interest of soil moisture and ocean salinity (SMOS) ESA mission (see for instance http://www.esa.int/esaLP/LPsmos.html) on using the IGS VTEC maps, including predicted products, a new initiative is starting.

Other modernization aspects foreseen for the IGS VTEC maps are the increase of temporal resolution (reducing the current temporal resolution of 2 hours, significantly higher than the actual temporal resolution used by several IAACs), and the recomputation campaign. Indeed, revisiting old datasets with new techniques is a must: As it has been shown in Table 1, the combined IGSG product during the last years is slightly better that any of the individual IAAC maps coinciding with the VTEC mapping technique update performed few years ago for several IAACs. And new improvements are incoming, including the potential generation of 3D electron content maps. In this context there is an ongoing campaign to reprocess all the individual IAAC VTEC maps since the service start, on June 1st 1998, but with the very latest technique implemented by each analysis center. This is expected to provide better VTEC maps, specially for the older datasets.

We would like to end the paper, emphasizing that an increasing time series of accurate global VTEC are available since 1998, which are freely available for scientific or technical usage, with latencies of about 12 days (final product) or still better (1-2 days) for rapid product (see for instance International GNSS Service Central bureau, http://www.igs.org), thanks to the cooperative effort developed within the IGS framework, and that this open service to the International Community will hopefully continue its evolution during the next years, sensitive to both new user needs and scientific achievements.

Acknowledgments The authors are grateful to the IGS community support in general and to different sponsors partially supporting their work for IGS, such as the Spanish project ESP2007-62676 for UPC authors.

References

Afraimovich EL, Astafyeva EI, Oinats AV, Yasukevich Yu. V, Zhivetiev IV (2006) Global electron content and solar activity: comparison with IRI modeling results, poster presentation at IGS Workshop, Darmdstadt, Germany, May

Astafyeva EI, Afraimovich EL, Oinats AV, Yasukevich Yu. V, Zhivetiev IV (2006) Global electron content as a new index of solar activity, 36th COSPAR Scientific Assembly. Held 16–23 July 2006, in Beijing, China

Belehaki A, Jakowski N, Reinisch BW (2003) Comparison of ionospheric ionization measurements over Athens using ground ionosonde and GPS-derived TEC values. Radio Sci 28(6):1105. doi:10.1029/2003RS002868

Bellanger E, Blanter EM, Le Mouel J-L, Shnirman MG (2002) Estimation of the 13.63-day lunar tide effect on length of day, J Geophys Res 107(B5):2102. doi:10.1029/2000JB000076

Bilitza D (2001) International Reference Ionosphere 2000. Radio Sci 36(2): 261–275

Coker C, Kronschnabl G, Coco DS, Bust GS, Gaussiran TL II (2001) Verification of ionospheric sensors. Radio Sci 36(6):1523–1529

Coster A, Komjathy A (2008) Space weather and the global positioning system. Space Weather 6:S06D04. doi:10.1029/2008SW000400

Dow JM, Neilan RE, Gendt G (2005) The International GPS Service (IGS): Celebrating the 10th Anniversary and Looking to the Next Decade. Adv Space Res 36(3):320–326. doi:10.1016/j.asr.2005.05.125, 2005

Fagundes PR, Pillat VG, Bolzan MJA, Sahai Y, Becker-Guedes F, Abalde JR, Aranha SL (2005) Observations of F layer electron density profiles modulated by planetary wave type oscillations in the equatorial ionospheric anomaly region. J Geophys Res 110:A12302. doi:10.1029/2005JA011115

Feltens J (1998) Chapman Profile Approach for 3-d Global TEC Representation, IGS Presentation. In: Proceedings of the 1998 IGS

analysis centers workshop, ESOC, Darmstadt, Germany, 9–11 February, pp 285–297

Feltens J (2007) Development of a new three-dimensional mathematical ionosphere model at European Space Agency/European Space Operations Centre. Space Weather 5:S12002. doi:10.1029/2006SW000294

Feltens J, Schaer S (1998) IGS Products for the Ionosphere, IGS Position Paper. In: Proceedings of the IGS analysis centers workshop, ESOC, Darmstadt, Germany, pp 225–232, 9–11 February

Gao Y, Heroux P, Kouba J (1994) Estimation of GPS receiver and satellite L1/L2 signal delay biases using data from CACS. In: Proceedings of KIS-94, pp 109–117, Banff, Canada, 30 August–2 September

Heelis RA, Coley WR (1992) East-west ion drifts at mid-latitutdes observed by dynamics explorer 2. J Geophys Res 97(A12):19461–19469

Hernández-Pajares M (2004) IGS Ionosphere WG status report: performance of IGS Ionosphere TEC Maps -Position Paper-, presented at IGS Technical Meeting, Bern, Switzerland

Hernández-Pajares M, Juan JM, Sanz J (1999) New approaches in global ionospheric determination using ground GPS data. J Atmos Sol Terr Phys 61:1237–1247

Hernández-Pajares M, Juan JM, Sanz J, Colombo OL (2000) Application of ionospheric tomography to real-time GPS carrier-phase ambiguities resolution, at scales of 400–1000 km and with high geomagnetic activity. Geophys Res Lett 27(13):2009–2012

Hernández-Pajares M, Juan JM, Sanz J (2008) GPS data processing: code and phase Algorithms, Techniques and Recipes. http://www.gage.es/TEACHING_MATERIAL/GPS_BOOK/ENGLISH/PDGPS/BOOK_PDGPS_gAGE_NAV_08.pdf, Barcelona, issue 2E, February

Mannucci AJ, Wilson BD, Yuan DN, Ho CH, Lindqwister UJ, Runge TF (1998) A global mapping technique for GPS-derived ionospheric total electron content measurements. Radio Sci 33:565–582

Orus R, Cander LR,2, Hernández-Pajares M (2007) Testing regional vertical total electron content maps over Europe during the 1721 January 2005 sudden space weather event, Radio Sci 42:RS3004. doi:10.1029/2006RS003515

Sardon E, Rius A, Zarraoa N (1994) Estimation of the transmitter and receiver differential biases and the ionospheric total electron content from Global Positioning System Observations. Radio Sci 29:577

Schaer S (1999) Mapping and Predicting the Earth's Ionosphere Using the Global Positioning System, Ph.D. Dissertation Astronomical Institute, University of Berne, Berne, Switzerland, 25 March

Schaer S (2003) IGS GLONASS tracking data. IGS Mail No. 4371, 8 May

Stening RJ, Fejer BG (2001) Lunar tide in the equatorial F region vertical ion drift velocity. J Geophys Res 106(A1): 221–226

Stening RJ, Richmond AD, Roble RG (1999) Lunar tides in the Thermosphere-Ionosphere-Electrodynamics General Circulation Model, J Geophys Res 104(A1):1–13

Wang X, Eastes R, Weichecki Vergara S, Bailey S, Valladares C, Woods T (2006) On the short-term relationship between solar soft X-ray irradiances and equatorial total electron content (TEC). J Geophys Res 111:A10S15. doi:10.1029/2005JA011488

Wilson BD, Mannucci AJ (1993) Instrumental biases in ionospheric measurements derived from gps data. In: Proceedings of the Institute of Navigation GPS-93, pp 1343–1351, September